Quantifying 10 Years of Improved Earthquake-Monitoring Performance in the Caribbean Region

by Daniel E. McNamara, Christa von Hillebrandt-Andrade, Jean-Marie Saurel, Victor Huerfano, and Lloyd Lynch

ABSTRACT

Over 75 tsunamis have been documented in the Caribbean and adjacent regions during the past 500 years. Since 1500, at least 4484 people are reported to have perished in these killer waves. Hundreds of thousands are currently threatened along the Caribbean coastlines. Were a great tsunamigenic earthquake to occur in the Caribbean region today, the effects would potentially be catastrophic due to an increasingly vulnerable region that has seen significant population increases in the past 40–50 years and currently hosts an estimated 500,000 daily beach visitors from North America and Europe, a majority of whom are not likely aware of tsunami and earthquake hazards. Following the magnitude 9.1 Sumatra–Andaman Islands earthquake of 26 December 2004, the United Nations Educational, Scientific and Cultural Organization (UNESCO) Intergovernmental Coordination Group (ICG) for the Tsunami and other Coastal Hazards Early Warning System for the Caribbean and Adjacent Regions (CARIBE-EWS) was established and developed minimum performance standards for the detection and analysis of earthquakes. In this study, we model earthquake-magnitude detection threshold and *P*-wave detection time and demonstrate that the requirements established by the UNESCO ICG CARIBE-EWS are met with 100% of the network operating. We demonstrate that earthquake-monitoring performance in the Caribbean Sea region has improved significantly in the past decade as the number of real-time seismic stations available to the National Oceanic and Atmospheric Administration tsunami warning centers have increased. We also identify weaknesses in the current international network and provide guidance for selecting the optimal distribution of seismic stations contributed from existing real-time broadband national networks in the region.

INTRODUCTION

In this document, we review earthquake and tsunami hazard in the Caribbean region, describe seismic monitoring efforts, and assess compliance with performance requirements established by the United Nations Educational, Scientific and Cultural Organization (UNESCO) Intergovernmental Coordinating Group (ICG) for the Tsunami and other Coastal Hazards Early Warning System for the Caribbean and Adjacent Regions (CARIBE-EWS) Working Group 1 (WG1) on Warning and Detection Systems (UNESCO Intergovernmental Oceanographic Commission [IOC], 2005; IOC, 2013).

The magnitude 9.1 Sumatra–Andaman Islands earthquake of 26 December 2004 increased global awareness of the destructive hazard posed by earthquakes and tsunamis. Postevent assessments of global coastline vulnerability highlighted the Caribbean as a region of high risk that was poorly monitored (von Hillebrandt-Andrade, 2013). Significant efforts to improve monitoring capabilities in the region have been undertaken since that time, including an expansion of the U.S. Geological Survey (USGS) Global Seismographic Network (GSN) (McNamara *et al.*, 2006) and organization of the UNESCO ICG CARIBE-EWS in 2005. Minimum seismic network-performance requirements established by the CARIBE-EWS WG1 for initial earthquake locations, and investigated in this study, include: (1) earthquake detection within 1 min and (2) minimum magnitude threshold of **M** 4.5.

In this study, we demonstrate that the development of an international cooperative virtual seismic network, from 2004 to 2014, has significantly lowered the earthquake-magnitude detection threshold and *P*-wave detection time throughout the region. We model these network-performance measures and demonstrate that the requirements established by the UNESCO ICG CARIBE-EWS WG1 are met with 100% of the network operating. Typically, seismic networks have only 80%–90% of the stations operational, and therefore station redundancy is required to consistently meet the UNESCO ICG CARIBE-EWS WG1 requirements. We also show coverage gaps in the current network that should be reinforced with additional stations to assure that the minimum requirements are continuously achieved for effective early warning.

Caribbean Earthquake and Tsunami Hazard

Significant progress has been made to improve earthquake and tsunami monitoring globally since the great 2004 earthquake and tsunami offshore of Sumatra. However, tsunamigenic events in the Atlantic and Caribbean are less frequent than

doi: 10.1785/0220150095

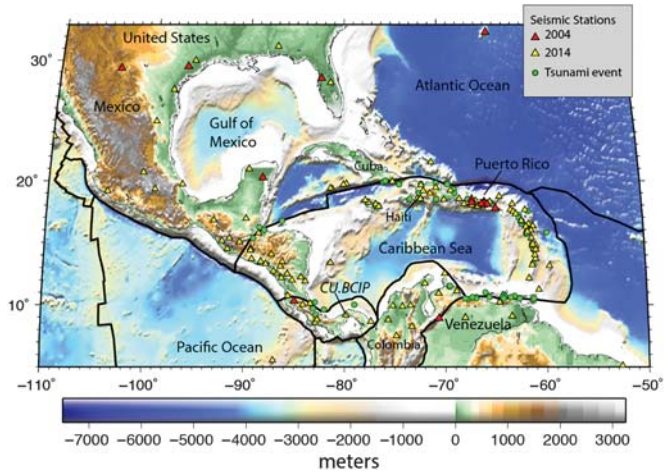

▲ **Figure 1.** Map of the Caribbean Intergovernmental Coordinating Group Tsunami and other Coastal Hazards Early Warning System for the Caribbean and Adjacent Regions earthquake-monitoring network used in the analysis presented in this article. Red triangles are seismic stations available to the Pacific Tsunami Warning Center (PTWC) and U.S. National Tsunami Warning Center (NTWC) in 2004. Yellow triangles show seismic stations added since 2004. Tectonic plate boundaries (black lines) are taken from Bird (2003) and represent potential tsunamigenic earthquake source zones. Green circles are earthquake and volcanic tsunamigenic events (von Hillebrandt-Andrade, 2013).

in other regions and not as well understood. The tsunami hazards for coastlines in the Gulf of Mexico, Atlantic Ocean, and Caribbean islands are unique in that practically all the known causes of tsunamis are present (Fig. 1) (von Hillebrandt-Andrade, 2013). For example, large submarine landslides pose significant tsunami hazard to Puerto Rico, along with earthquakes (ten Brink and Lin, 2004; ten Brink *et al.*, 2009), whereas volcano-triggered tsunamis threaten the Lesser Antilles (Zahibo *et al.*, 2005; Hayes *et al.*, 2014). Earthquake and tsunami hazards in the Caribbean have been the topic of many studies over the past 30 years, primarily focusing on the northern Caribbean plate boundary and the Lesser Antilles (e.g., Stein *et al.*, 1982; McCann and Sykes, 1984; Bernard and Lambert, 1988; Calais *et al.*, 1998; Dolan and Wald, 1998; DeMets *et al.*, 2000; Mann *et al.*, 2002, 2005; Geist and Parsons, 2009; Geist *et al.*, 2009; Parsons and Geist, 2009; ten Brink *et al.*, 2009; Hayes *et al.*, 2010; Lopez-Venegas *et al.*, 2015).

Over 75 tsunamis have been reported for the Caribbean region in the past 500 years (von Hillebrandt-Andrade, 2013), including 14 tsunamis reported in Puerto Rico and the U.S. Virgin Islands. In this time, 30 tsunamis caused significant damage and as many as 4484 recorded fatalities (National Oceanic and Atmospheric Administration National Geophysical Data Center [NOAA NGDC], see Data and Resources). During the past 150 years, nearly 2150 deaths were attributed to tsunamis in the Caribbean. The death toll due to tsunamis impacting the combined coasts of Hawaii, Alaska and California, Oregon and Washington is five times less than in the Caribbean for the same time period (Proenza and Maul, 2010).

In 1946, an **M** 8.1 earthquake north of Hispaniola generated a tsunami that killed a reported 1790 people in the region (NOAA NGDC, see Data and Resources). More recently, on 21 November 2004, a strong and shallow (M_w 6.3, 14 km depth) earthquake occurred in the Les Saintes Passage that separates Guadeloupe from Dominica, in the Lesser Antilles. Strong shaking, with intensities as high as VII, was reported, and the earthquake generated a tsunami with maximum runup amplitudes of 70–80 cm on neighboring islands (Zahibo *et al.*, 2005).

In January 2010, the devastating M_w 7.0 Haiti earthquake (Hayes *et al.*, 2010), triggered independent twin tsunamis along the coastlines inside the Gulf of Gonave and along Haiti's south coast, resulting in wave-induced flooding and damage to coastal infrastructure. The tsunami waves caused at least three fatalities at Petit Paradis inside the Gulf of Gonave due to a complete lack of tsunami awareness (Hornbach *et al.*, 2010). Fritz *et al.* (2013) documented tsunami runup observations along 100 km of the Hispaniola southern coast. The tsunami impact peaked with maximum tsunami heights exceeding 3 m at Jacmel on Haiti's south coast, and tsunami runup of more than 1 m was observed at Pedernales in the Dominican Republic. The tsunami was well recorded in the open ocean at Deep-ocean Assessment and Reporting of Tsunamis (DART) buoy 42407, 600 km southeast (amplitude 0.4 cm). In addition, the Santo Domingo tide gauge, located 300 km east of the earthquake source, recorded the tsunami (about one hour after the earthquake), with an amplitude of 5 cm and spectral periods of 500 s and greater (Fritz *et al.*, 2013).

Though the majority of the large damaging earthquakes in the Caribbean have occurred within the northern plate boundary zone, the relatively less complex subduction zone of the Lesser Antilles arc further south has also hosted such earthquakes in the past, most notably in 1843 when an **M** 7.5–8.5 earthquake killed several thousand people on Guadeloupe and surrounding islands (Robson, 1964). Another great Lesser Antilles subduction zone earthquake, as forecast in numerous studies (McCann and Sykes, 1984; Bernard and Lambert, 1988; Hayes *et al.*, 2014), could be of a depth and mechanism sufficient to produce a significant local tsunami. Such a "short-fuse" tsunami would provide very little lead time for the local island communities to respond (Proenza and Maul, 2010).

In addition to local earthquake and tsunami risk, an earthquake along the northern or eastern Caribbean plate boundary zones poses a potential threat to the greater Atlantic basin through a transoceanic tsunami. The subduction zones of the Caribbean are the closest convergent plate boundaries to the eastern coasts of North and South America and the western coasts of Europe and Africa (Mann *et al.*, 2002, 2005; Geist and Parsons, 2009; Parsons and Geist, 2009). Were a great tsunamigenic earthquake to occur in the Caribbean region today, the effects would potentially be catastrophic due to an increasingly vulnerable region that has seen significant population increases in the past 40–50 years (G. Hyman, see Data and Resources) and currently hosts an estimated 500,000 daily beach visitors from North America and Europe, a majority of whom

are not likely aware of tsunami and earthquake hazards (Proenza and Maul, 2010).

Earthquake-Monitoring Networks

An efficient and effective tsunami early warning system requires seismic, sea-level, and other observational data that must be available and processed in a reliable and timely manner. Since the 2004 Sumatra–Andaman earthquake, tsunami global efforts have been undertaken to ensure that vulnerable coastlines are better prepared for a tsunami. Since 2006, the U.S. National Weather Service (NWS) Pacific Tsunami Warning Center (PTWC) in Hawaii has provided an interim service to the Caribbean region, whereas the U.S. National Tsunami Warning Center (NTWC) in Palmer, Alaska, provides service for Puerto Rico and the Virgin Islands. In 2010, the NWS established the Caribbean Tsunami Warning Program (CTWP) in Mayagüez, Puerto Rico. The CTWP supports an increased capability of the tsunami observational system and the continued enhancement of tsunami outreach and education capacity. Numerous local, national, and regional seismic networks monitor earthquake activity in the region. Data are also available from the adjoining regions, mainly from the global seismic networks. Here, we focus on earthquake-monitoring systems in the region.

ICG CARIBE-EWS Seismic Network

When the ICG first met in 2006, only 10 stations in the Caribbean region were used by the tsunami warning centers (TWCs). High-quality existing seismic stations that are components of individual national networks were combined into a virtual real-time network that currently contributes real-time data to the TWCs and archived at the Incorporated Research Institutions for Seismology (IRIS) Data Management System. Primary original contributors include: the Puerto Rico Seismic Network (PRSN) (Clinton *et al.*, 2006), the USGS GSN (McNamara *et al.*, 2004), GEOSCOPE (Roult and Montagner, 1994; Stutzmann *et al.*, 2000), University of the West Indies Seismic Research Center, GEOFON (Hanka and Kind, 1994), the IRIS GSN network, and stations operated by the Comprehensive Nuclear-Test-Ban Treaty Organization. Based on the continuing coordination efforts by the PRSN and CTWP, significantly more seismic stations are currently available to the TWCs. In 2014, over 100 seismic stations, from nearly every nation of the Caribbean region, contribute real-time seismic data to the TWCs (Fig. 1). More recent significant national network contributors include Cuba, Mexico, Colombia, Venezuela, Nicaragua, Costa Rica, the Cayman Islands, Haiti, Jamaica, Guatemala, the Netherlands, Aruba, and Curaçao. We show significant improvement in earthquake and tsunami monitoring performance from 2004 to 2014 due to the contributions of real-time seismic data from most nations in the Caribbean region.

METHODS FOR MODELING SEISMIC NETWORK PERFORMANCE

Here, we present methods for modeling seismic network performance. The methods are unique in that each is dependent on the ambient noise levels and distribution of individual stations. The two network-performance measures described in this report are (1) moment magnitude (M_w) earthquake detection threshold and (2) *P*-wave detection time. These measures of network performance are routinely used at the USGS National Earthquake Information Center (NEIC) and GSN to assess the real-time monitoring performance of the automated earthquake detection and location systems (McNamara *et al.*, 2004).

M_w Threshold Method

Characterizing the frequency-dependent noise levels at individual broadband stations is the first essential step in quantifying the performance of a seismic network. Noise levels are determined for each station in the network using long-term distributions of power spectral density (PSD) (McNamara and Buland, 2004). We use the *PQLX* software system to compute PSD probability density functions (PDFs) (McNamara and Boaz, 2011) for all continuous vertical-component channels. With this approach, there is no need to screen for system transients, earthquakes, and general data artifacts, because they map into a low background probability level. *P*-wave detection for small-magnitude earthquakes (**M** 2–4) is most sensitive to noise levels in the 0.5–10 Hz frequency band, which is dominated by cultural noise sources such as cars and machinery and high-frequency modes associated with the oceanic microseism (McNamara and Buland, 2004). Figure 2 shows the variation of the vertical-component PSDPDF distributions used to determine the individual station baseline ambient noise levels (McNamara *et al.*, 2009) required to model the network M_w detection threshold.

For an earthquake to be detected in our model, spectral acceleration (after Brune 1970, 1971) must exceed long-term seismic-station median noise levels, at the appropriate source corner frequency. We compute the M_w detection threshold on a grid of 1° cells. For each grid cell, we calculate distance Δ to each seismic station (Fig. 3a). For each cell–station path, we step through a range of source corner frequencies (f_c) and compare the modeled spectral amplitude to the station median noise level. For each f_c, we compute moment (M_0) after Brune (1970, 1971), in which

$$M_0 = 2.29\sigma r^3 \text{ dyn} \cdot \text{cm}. \quad (1)$$

We assume an effective stress drop $\sigma = 1.0 \times 10^7$ Pa (10 MPa), and the fault radius r is

$$r = \frac{2.21\beta}{2\pi f_c} \text{ cm}. \quad (2)$$

We assume a shear-wave velocity $\beta = 3.5$ km/s and find angular frequency f_m, by bisection, in which the Brune source spectrum is a maximum, given a standard detection filter (0.5–12 Hz).

We then calculate *S*-wave amplitude A_S due to the Brune source model, distance Δ, and standard short-period detection filters:

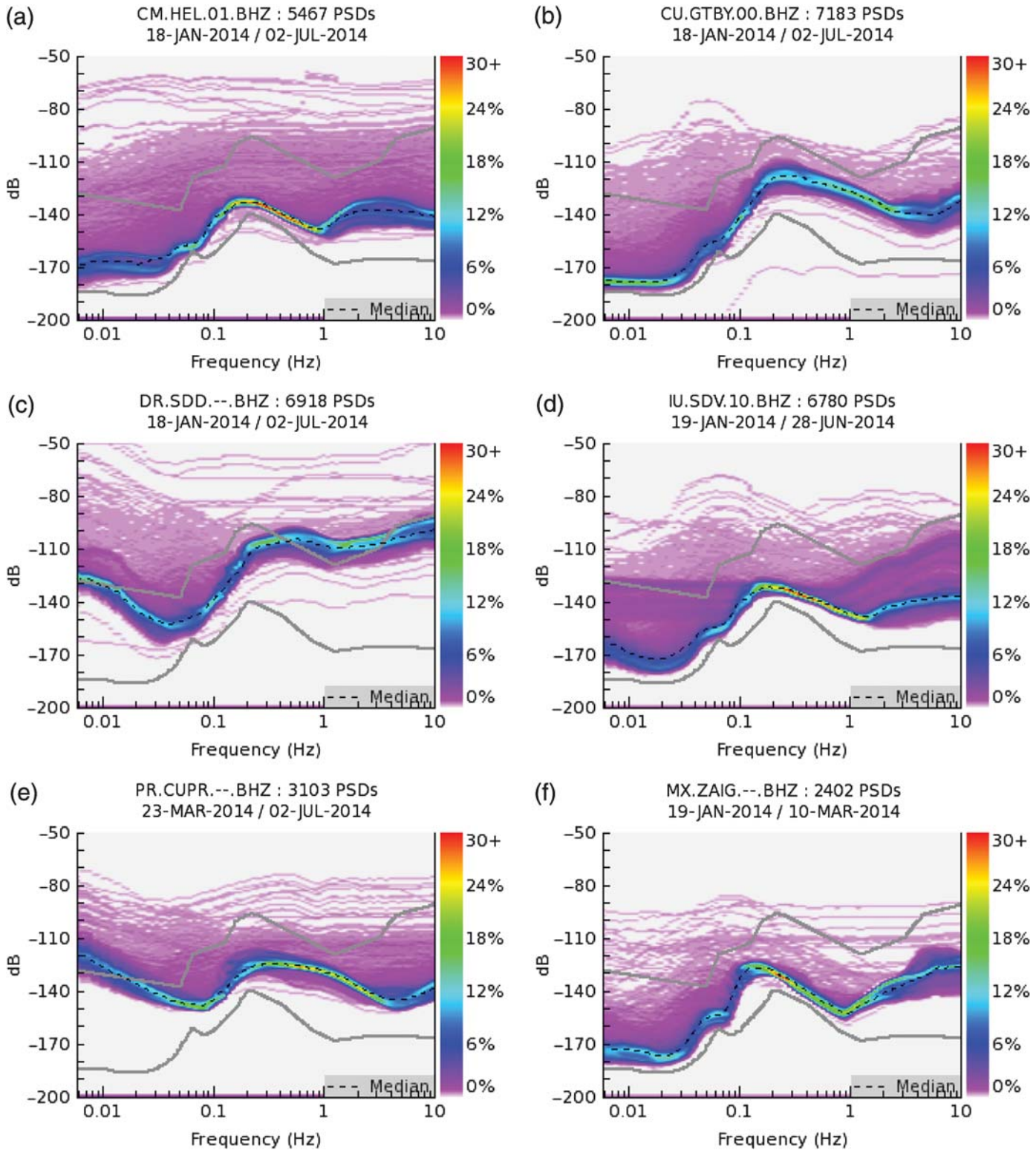

▲ **Figure 2.** Power spectral density (PSD) probability density functions (PDFs) and median noise levels (dashed black line) for six stations used in this analysis are shown. (a) CM.HEL.01.BHZ from the Colombia national network. (b) CU.GTBY.00.BHZ, U.S. Geological Survey (USGS) Global Seismographic Network (GSN) in Guatanamo Bay, Cuba. (c) DR.SDD.–.BHZ, in the Dominican Republic. (d) IU.SDV.10.BHZ USGS GSN in Venezuela. (e) PR.CUPR.–.BHZ, Puerto Rico Seismic Network (PRSN) in Puerto Rico. (f) MX.ZAIG.–.BHZ contributed from the Mexico national network. *P*-wave detection for the small magnitudes modeled in this study is most sensitive to the 0.5–10 Hz frequency band. Gray lines are high and low noise models (Peterson, 1993).

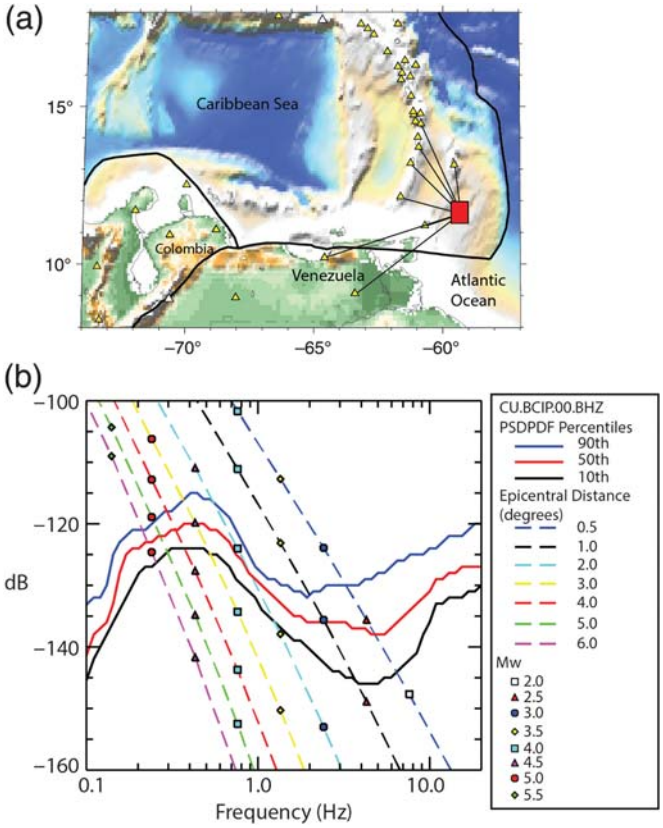

▲ **Figure 3.** M_w detection-threshold method illustration. (a) Map showing example 1° grid cell (red square) and paths (black lines) to detecting seismic stations (yellow triangles). (b) PSDPDF noise level examples for station CU.BCIP, the USGS GSN station in Panama. The 90th, 50th (median), and 10th percentile of the PSDPDF versus *P*-wave amplitude (dB) along several distance paths (0.5°–6.0°) for a range magnitudes (**M** 2.0–5.5) are shown.

$$A_S = \frac{M_0}{4\pi\beta} \times \frac{f_m f_c}{f_m} + \frac{f_c^2}{\Delta}. \quad (3)$$

(Brune, 1970, 1971) in which μ is rigidity.

To take into account path effects, we apply an appropriate Q and geometrical spreading terms γ to the A_s.

$$A_S = \frac{A_S}{\Delta^\gamma} e^{\frac{-\pi f_m \Delta}{Q\beta}} \quad (4)$$

We assume a distance-dependent geometrical spreading γ, such that if $\Delta < 70$ km, then $\gamma = -1.0$; if $\Delta = 70$–150 km, then $\gamma = 1.1$; and if $\Delta > 150$ km, then $\gamma = 0.5$ (Motazedian and Atkinson, 2005). We apply a frequency-dependent Q function determined for the Hispaniola region to represent the attenuation characteristics of the Caribbean island arc environment ($Q(f) = 224f^{0.64}$; McNamara *et al.*, 2012).

Next, we compute *P*-wave amplitude (A_P) from modeled Brune A_S using standard S/P ratios ($A_P = A_S/3.0$ after McGinley and Anderson, 1969). *P*-wave amplitude is then converted to power (P) in decibels with $P = 10\log(A_P^2/\text{Hz})$ and compared to the median seismic-station noise level at f_c. If A_P is greater than the median noise level at f_c, a successful detection is declared (Fig. 3b).

The minimum M_w for each model grid cell is then determined by the smallest M_w at the third detecting station, after Kanamori (1977):

$$M_w = 0.667\log(M_0) - 10.7. \quad (5)$$

TWC procedures require three stations for detection globally. Modeled earthquake seismic-wave spectral amplitudes are then compared to the median noise level at every station in the network to determine a grid of minimum detectable M_w.

Each cell in the detection-threshold model represents the smallest earthquake that can be detected by the smallest M_w at the third detecting station used in the simulation (Fig. 3). The third station is used because the TWCs require three stations to declare an automatic earthquake detection. The stations included in the earthquake solution are determined by the signal-to-noise level and not necessarily due to the proximity of the earthquake source to the recording station. Nearby stations with high noise levels may not detect the smallest magnitude events and thereby increase the detection-threshold magnitude.

Figure 3b shows a range of magnitude–distance pairs and demonstrates how different noise levels can affect the detection threshold. For this study, we assume the median of the PSDPDF distribution, which approximates a 50% probability of detection. Details on noise level selection and calibration are described in the Discussion section. Figure 3 graphically demonstrates the method for a single grid cell. Figures 4a and 5a show modeled results where the minimum detectable earthquake M_w is mapped at each grid cell for station distributions available in 2004 and 2014 (Figs. 4a and 5a).

P-Wave Detection-Time Method

The *P*-wave detection-time modeling method computes the travel time of the first arriving *P* wave, using the *Tau-P* method and the IASPEI91 Earth model (Buland and Chapman, 1983), to the third station that detected the minimum M_w earthquake determined in the global detection grid. This approach gives us a worst-case scenario, because it models the *P*-wave detection time of the smallest detectable earthquake. If larger earthquakes are modeled, propagation times are smaller, because the events are more likely to be detected on seismic stations with high noise conditions. The modeled detection-time grid gives a sense of the network configuration relative to the spatial distribution of the earthquake source zones (Figs. 4b and 5b). The *P*-wave detection-time model should not be considered an absolute measure of response time, but instead is the delay time required before the TWCs can begin computing an earthquake location and magnitude. Additional time is required for automated systems to compute the initial earthquake location and magnitude before a warning can be issued.

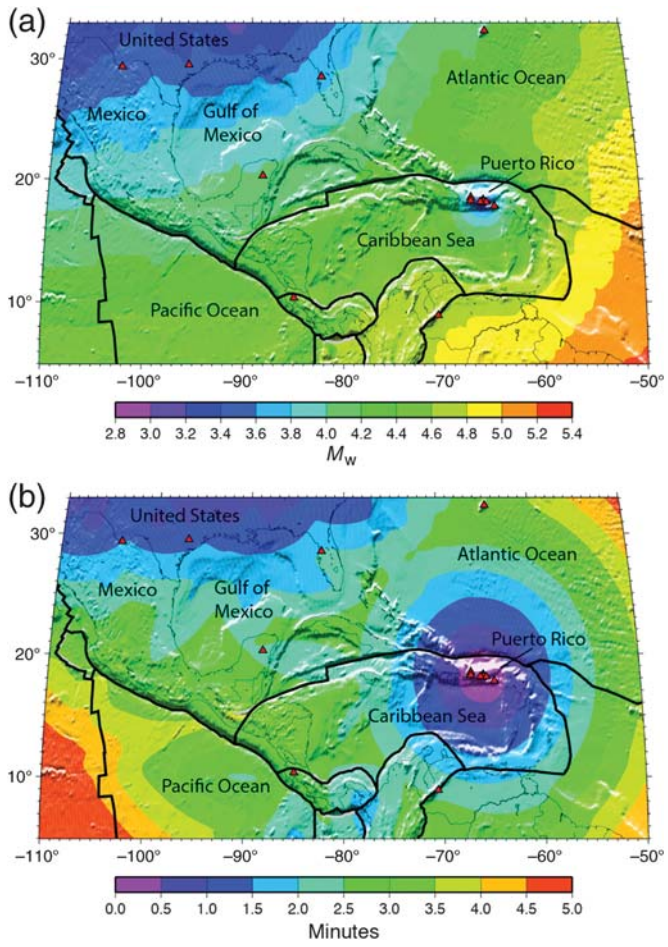

▲ **Figure 4.** 2004 seismic network-performance models. (a) M_w detection threshold. (b) *P*-wave detection time. Red triangles are seismic stations available to the PTWC and NTWC in 2004. Tectonic plate boundaries (black lines) are taken from Bird (2003).

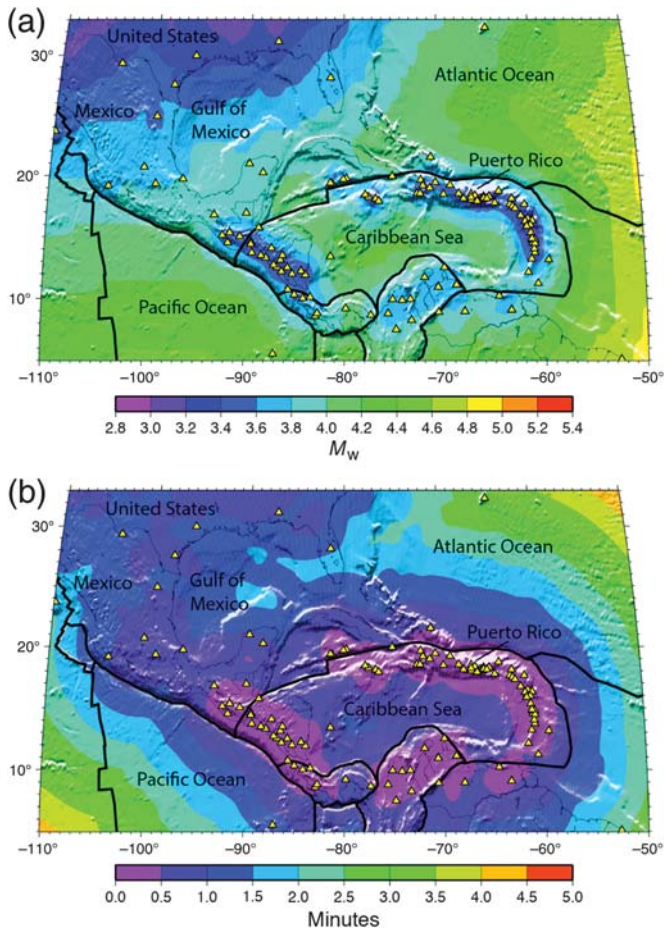

▲ **Figure 5.** 2014 seismic network-performance models. (a) M_w detection threshold. (b) *P*-wave detection time. Yellow triangles are seismic stations available to the PTWC and NTWC in 2014.

DISCUSSION

Here, we discuss results from the two measures of seismic network performance modeled for the distribution of seismic stations available to the PTWC and NTWC in the years 2004 and 2014. As seen in Figure 4, in 2004 very few seismic stations in the area were available to the TWCs; and, consequently the seismic network-performance standards, required by WG1, were poorly met throughout the region. The exception was in the vicinity of Puerto Rico, where earthquakes with $\mathbf{M} < 3$ could be detected in less than one minute. Outside of the Puerto Rico region, *P*-wave detection time was on the order of several minutes for $\mathbf{M} > 4$ earthquakes.

As of 2014, the real-time seismic stations available to the NOAA TWCs nearly meet the performance standards established by WG1 (Fig. 5). Recent network additions since 2004 (Nicaragua, Colombia, Mexico, Cayman Islands, Venezuela, and Jamaica) have reduced detection threshold and detection time throughout much of the Caribbean region and Central America. For example, Figure 5 shows that, throughout all of the seismogenic zones of the Caribbean, earthquakes with magnitude 3 and larger can be detected within 1 min. Exceptions to this are northern South America and portions of Mexico.

Throughout a given year, ambient noise levels can change due to seasonal variation of the microseism and thereby have an effect on earthquake detection threshold (Aster *et al.*, 2008). This is reflected in the range between the 10th and 90th percentile noise levels from 0.1 to 1.0 Hz, shown in Figure 3b. As a result, M_w detection can vary by approximately $+0.5$ M_w. In this study, we use median noise levels at each station that are not sensitive to the seasonal noise variations.

Direct calibration of the M_w detection threshold and *P*-wave detection-time models is not easily accomplished, because there are many variable assumptions in the methods. In addition, earthquake catalogs used for calibration are limited throughout the Caribbean region. We have attempted to make the appropriate variable selections based on the standard operating procedures of the TWCs and based on several years of application at the USGS NEIC. Because the PRSN has the most complete catalog in the region, it is used here to calibrate the models.

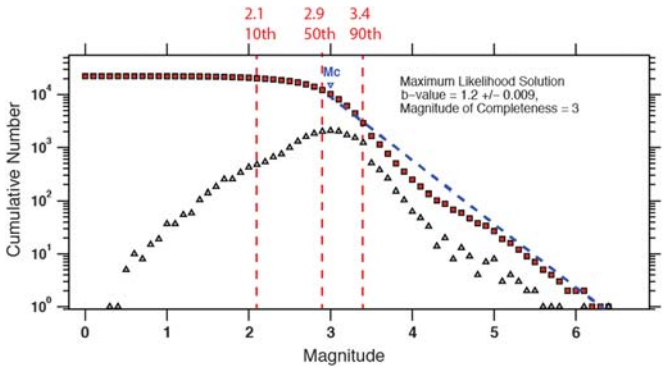

▲ **Figure 6.** PRSN earthquake catalog magnitude–frequency distribution showing the magnitude of completeness and *b*-value results. Red squares represent the cumulative number of earthquakes in each bin, whereas gray triangles are the actual number of earthquakes. The total catalog (2004–2014) median magnitude is **M** 2.9, with $M_c = 3.0$ determined by the maximum curvature of the cumulative bins. A *b*-value of 1.2 was determined for magnitudes greater than $M_c > 3$ using a maximum-likelihood method and is slightly higher than global average ($b = 1$).

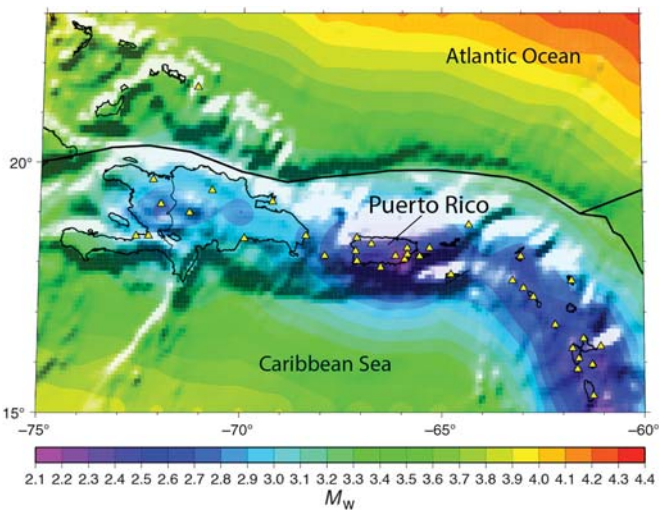

▲ **Figure 7.** The Puerto Rico region showing M_w threshold network-capability model assuming PSDPDF for the 10th percentile noise levels for each seismic station. The M_w threshold in Puerto Rico, assuming PSDPDF for the 10th percentile noise levels, is as low as M_w 2.1, which matches the 10th percentile of the 10 yr PRSN catalog magnitude distribution (Fig. 6). Yellow triangles are seismic stations available to the PTWC and NTWC in 2014.

M_w Threshold Calibration

In this section, we attempt to calibrate the minimum M_w detection-threshold models by comparison with the PRSN earthquake catalog (Fig. 6). Over 22,000 earthquakes were detected from 2004 to 2014 by the PRSN. The median of the PRSN magnitude distribution is **M** 2.9 (Fig. 6) with a magnitude of completeness of $M_c = 3.0$ and *b*-value of $b = 1.2$ (Fig. 6). The minimum magnitude earthquake detection modeled in the PRSN region of **M** 2.8–3.0 (Fig. 5a) is roughly consistent with the median magnitude (**M** 2.9) in the PRSN catalog (Fig. 6). Using the 50% PSDPDF (median) noise level in the M_w detection-threshold model therefore approximates the 50% probability of detection. Similarly, assuming a significantly lower 10% PSDPDF noise level approximates a 10% probability of detection (**M** ~ 2.1) (Fig. 7). We observe that PSDPDF noise level is related to the PRSN catalog magnitude distribution and approximates a probability of detection.

P-Wave Detection-Time Calibration

Because the station distribution used in the *P*-wave detection-time model is determined by the M_w threshold model we also suggest that the model represents a certain probability of detection based on the selected noise level. Models in Figures 4b and 5b represent a 50% probability of detecting a *P* wave within the modeled time because the 50th percentile noise levels were used for each station.

Ten Years of Monitoring Performance Improvement

Although absolute values are not well calibrated, we can nevertheless look at differences between models to examine changes in network performance through time. In Figure 8, a map of the difference between 2004 and 2014 models shows the significant improvement in both performance measures over the 10 yr period. For example, the minimum detectable magnitude was lowered by over 1 unit in the Lesser Antilles, South and Central America, and in the vicinity of Haiti and the Dominican Republic. It is not surprising that there is little improvement (**M** ~ 0.1) in the Puerto Rico region, because there were already a good number of stations available in 2004 (Fig. 8a). Significant improvements of several minutes in *P*-wave detection time (Fig. 8b) are observed for earthquakes in Central America and of more than 1 min in the Lesser Antilles, South America, and Hispaniola region. Because the first ICG meeting in 2006, the deployment of modern broadband seismic stations and the sharing of existing data have allowed significant improvements in the seismic network capabilities modeled in this study (Fig. 8).

Seismic Network-Performance Sensitivity to Station Outages

Results from our modeling and PRSN catalog calibration analysis suggest that requirements of the ICG WG1 are currently met with 100% station operation. Typically, seismic networks operate with only 80%–90% of the available stations, and therefore redundancy is required to consistently meet WG1 requirements. Redundancy is critical to avoid data outages due to communication problems, vandalism, extreme weather, aging hardware, and other possible failure scenarios. This is especially true in the event of a destructive earthquake and/or tsunami when weaknesses in the system most likely cause points of failure. For this reason, the focus should turn to identifying vulnerabilities and weaknesses in the system to fortify the network.

The NOAA CTWP generates monthly statistics on the operational components of the network. In 2013, an average of only 78% of the stations contributed, with more than 90% of data availability within a minute. To approximate realistic

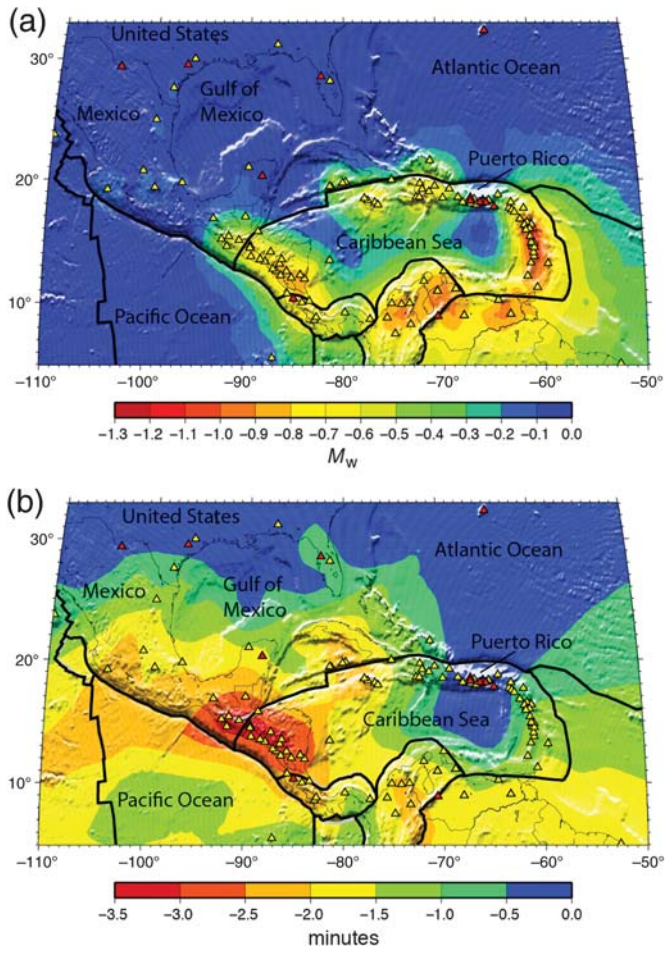

▲ **Figure 8.** Seismic network-performance maps showing the difference between 2004 and 2014 for seismic network improvements. (a) M_w detection threshold. (b) *P*-wave detection time. Red triangles are seismic stations available to the PTWC and NTWC in 2004. Yellow triangles show seismic stations added since 2004.

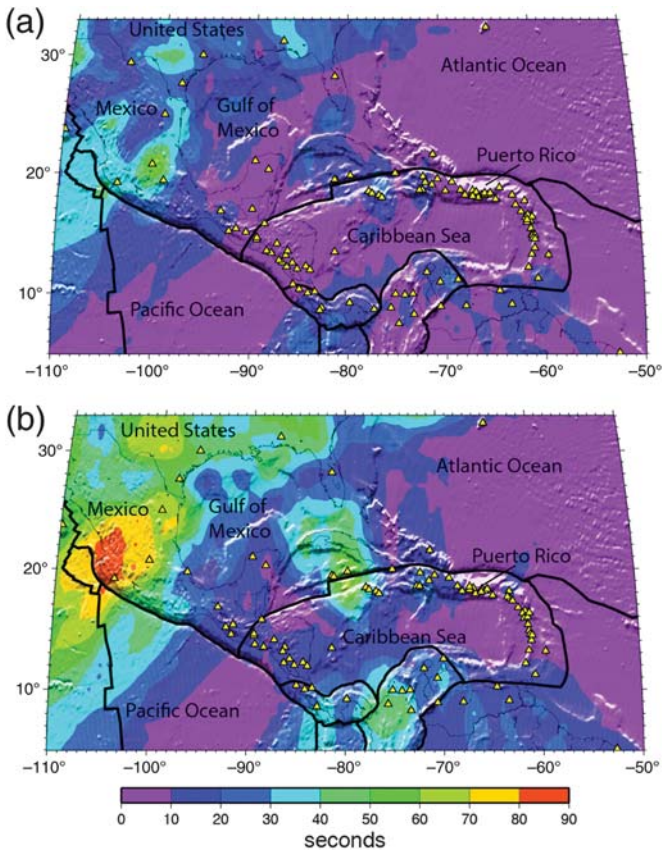

▲ **Figure 9.** Seismic network-performance sensitivity based on station distribution. Bootstrap approach showing the variance in *P*-wave detection time over 100 different models, assuming 10% and 25% station outage. *P*-wave detection-time variance is highest in regions where station density is lowest such as Mexico, Colombia, and Cuba. (a) 10% of network stations removed. (b) 25% of network stations removed. Yellow triangles show seismic stations added since 2004. Tectonic plate boundaries (black lines) are taken from Bird (2003).

station downtime and identify possible weaknesses in the network, we compute the variance *P*-wave detection time, assuming 100 different random network configurations with only 90% and 75% station operation, thus simulating, respectively, 10% and 25% network downtime. Figure 9a shows that a 10% network downtime affects mainly northern South America and the Jamaica/Cuba region. With 25% of stations not complying with the data availability criteria (Fig. 9b), the affected region extends to Hispaniolia and parts of Central America, the most affected regions being Jamaica/Cuba and the Colombia–Panama border. Low *P*-wave detection-time variance occurs where the network is generally dense, and high variance occurs in regions of relatively low station density. This type of information is useful for network operators by identifying regions where a single station failure may have a significant detrimental influence on network performance. Additional stations are needed in these regions to reinforce network performance.

The analysis of *P*-wave detection-time sensitivity to station density shown in Figure 9 provides constraints on which regions of the Caribbean should be considered for additional seismic stations. Station coverage gaps are identified in Mexico, northern Colombia, Panama, Honduras, Guatemala, Yucatán Peninsula, Cuba, and the Jamaica/Haiti region. In addition, due to the limited distribution of islands, permanent ocean-bottom observatories should be considered to fill gaps in the existing land-based seismic network. For example, the recent opening of relations with Cuba have resulted in seismic data sharing that will improve TWC *P*-wave detection time along the western end of the northern Caribbean plate boundary.

Seismic Network-Performance Sensitivity to National Network Outages

Station outages may not simply occur randomly, but instead complete networks can go down due to communication problems. In this section, we examine the impact of a complete network outage. The national seismic network of Venezuela (Fundación Venezolana de Investigaciones Sismológicas

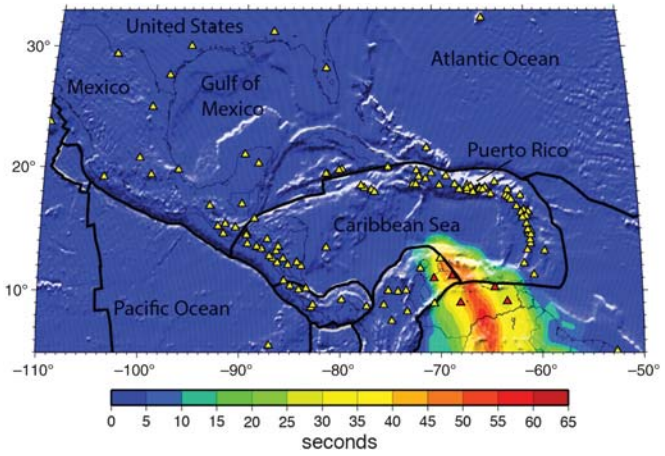

▲ **Figure 10.** Map of the difference in *P*-wave detection time between the complete network and when a single network (Fundación Venezolana de Investigaciones Sismológicas [FUNVISIS]) is removed. An increase in *P*-wave detection time of 30–60 s in Venezuela is observed due to the loss of five real-time seismic stations (red triangles) operated by FUNVISIS. Yellow triangles show seismic stations available to the TWCs in 2014. Tectonic plate boundaries (black lines) are taken from Bird (2003).

[FUNVISIS]) operates a large number of stations and within the past few years began contributing five of these stations to the PRSN and NOAA TWCs in real time. The addition of these five real-time stations has improved earthquake and tsunami monitoring capabilities in the northern South America region (Fig. 5). Figure 10 shows an example of the degradation in *P*-wave detection time, assuming the loss of all five FUNVISIS stations. Removing the FUNVISIS stations results in an increased *P*-wave detection time of nearly 40–60 s. This degradation in *P*-wave detection time would compromise the monitoring capability of the NOAA TWCs by significantly increasing warning times along the northern coast of South America. This example illustrates the importance of FUNVISIS as a member of the international monitoring network and the need for robust network data-sharing infrastructure in general.

CONCLUSIONS

Earthquake-monitoring performance in the Caribbean Sea region has improved significantly in the past decade as the number of real-time seismic stations available to the NOAA TWCs has increased. In this study, we model network-performance measures and demonstrate that the requirements established by the UNESCO ICG CARIBE-EWS WG1 are met with 100% of the network operating. The two measures of seismic network performance modeled in this study are (1) minimum M_w detection threshold and (2) *P*-wave detection time of an automatic processing system. By modeling network-performance measures, we demonstrate significant improvement in earthquake-monitoring performance as reduced earthquake-magnitude detection threshold and *P*-wave detection time throughout the region from 2004 to 2014.

We also identify weaknesses in the current international network and provide guidance for selecting the optimal distribution of seismic stations contributed from existing real-time broadband national networks in the region. Typically, seismic networks have only 80%–90% of the stations operational; therefore, station redundancy is required to consistently meet the UNESCO ICG CARIBE-EWS WG1 requirements. We also show coverage gaps in the current network that should be reinforced with additional stations to assure that the minimum requirements are continuously achieved for effective early warning. Although significant progress has been made to improve earthquake monitoring in the region, more can be done to strengthen the monitoring network by adding redundant stations in regions of weak coverage.

DATA AND RESOURCES

Earthquake source parameters used for detection-threshold model calibration were obtained from the Puerto Rico Seismic Network (http://redsismica.uprm.edu/English/, last accessed December 2014). All waveform data used in this study were obtained from the numerous national and regional networks in the Caribbean region and are archived and available for download from the Incorporated Research Institutions for Seismology Data Management Center. PQLX software was used to compute ambient noise statistics (McNamara and Boaz, 2011) (http://pubs.usgs.gov/of/2010/1292/, last accessed July 2014). G. Hyman's 2005 population database (Centro Internacional de Agricultura Tropical [CIAT], United Nations Environment Program [UNEP], Center for International Earth Science Information Network [CIESIN], Columbia University, and the World Bank Latin American and Caribbean Population Database v.3) is available from http://www.na.unep.net/datasets/datalist.php3 or http://gisweb.ciat.cgiar.org/population/dataset.htm (last accessed July 2014). The National Oceanic and Atmospheric Administration National Geophysical Data Center's NOAA/WDS Global Historical Tsunami Database is available at http://www.ngdc.noaa.gov/hazard/tsu_db.shtml (last accessed July 2014).

Network-performance modeling software was written by the authors. Generic Mapping Tool was used to generate maps and figures (Wessel *et al.*, 2013), and seismap was used for earthquake frequency–magnitude distribution calculations (Wiemer, 2002).

ACKNOWLEDGMENTS

This research was supported by the U.S. Geological Survey (USGS) National Earthquake Hazards Reduction Program. The authors thank all seismic network contributors in the region, including R. Pujols (Dominican Republic Seismic Network [DRSN]), G. Romero (Fundación Venezolana de Investigaciones Sismológicas [FUNVISIS]), Alberto Lopez and Elizabeth Vanacore (University of Puerto Rico-Mayagüez/Geology Puerto Rico Seismic Network) and all others. Important contributions were made by C. McCreary (National

Oceanic and Atmospheric Administration [NOAA] Pacific Tsunami Warning Center); P. Whitmore (NOAA National Tsunami Warning Center); B. Proenza (NOAA U. S. National Weather Service); P. Earle, G. Hayes, H. Benz, R. Buland, L. Gee, J. Weaver (USGS); B. Aliaga, Diana Patricia Mosquera (United Nations Educational, Scientific and Cultural Organization); and Lorna Inniss. The authors thank J. Braunmiller, an anonymous *SRL* reviewer, D. Wilson, and J. McCarthy for editorial and critical reviews. Any use of trade, product, or firm names is for descriptive purposes only and does not imply endorsement by the U.S. Government.

REFERENCES

Aster, R., D. McNamara, and P. Bromirski (2008). Multi-decadal climate-induced variability in microseisms, *Seismol. Res. Lett.* **79,** no. 2, 194–202, doi: 10.1785/gssrl.79.2.194.

Bernard, P., and J. Lambert (1988). Subduction and seismic hazard in the northern Lesser Antilles: Revision of the historical seismicity, *Bull. Seismol. Soc. Am.* **78,** 1965–1983.

Bird, P. (2003). An updated digital model of plate boundaries, *Geochem. Geophys. Geosyst.* **4,** no. 3, 1027, doi: 10.1029/2001GC000252.

Brune, J. (1970). Tectonic stress and the spectra of seismic shear waves from earthquakes, *J. Geophys. Res.* **75,** 4997–5009.

Brune, J. (1971). Correction, *J. Geophys. Res.* **76,** 5002.

Buland, R., and C. H. Chapman (1983). The computation of seismic travel times, *Bull. Seismol. Soc. Am.* **73,** 1271–1302.

Calais, E., J. Perrot, and B. Mercier de Lépinay (1998). Strike-slip tectonics and seismicity along the northern Caribbean plate boundary from Cuba to Hispaniola, *Geol. Soc. Am. Spec. Pap.* **326,** 125–142.

Clinton, J., G. Cua, V. Huérfano, C. von Hillebrandt-Andrade, and J. Martinez Cruzado (2006). The current state of seismic monitoring in Puerto Rico, *Seismol. Res. Lett.* **77,** 532–543.

DeMets, C., P. E. Jansma, G. S. Mattioli, T. H. Dixon, F. Farina, R. Bilham, E. Calais, and P. Mann (2000). GPS geodetic constraints on Caribbean–North America plate motion, *Geophys. Res. Lett.* **27,** 437–440.

Dolan, J. F., and D. J. Wald (1998). The 1943–1953 north-central Caribbean earthquakes: Active tectonic setting, seismic hazards, and implications for Caribbean–North America plate motions, *Geol. Soc. Am. Spec. Pap.* **326,** 143–170.

Fritz, H.M., J. V. Hillaire, E. Moliere, Y. Wei, and F. Mohammed (2013). Twin tsunamis triggered by the 12 January 2010 Haiti earthquake, *Pure Appl. Geophys.* **170,** nos. 9/10, 1463–1474.

Geist, E. L., and T. Parsons (2009). Assessment of source probabilities for potential tsunamis affecting the U.S. Atlantic Coast, *Marine Geol.* **264,** 98–108, doi: 10.1016/j.margeo.2008.08.005.

Geist, E. L., T. Parsons, U. S. ten Brink, and H. J. Lee (2009). Tsunami probability, in *The Sea*, E. N. Bernard and A. R. Robinson (Editors), Vol. 15, Harvard University Press, Cambridge, Massachusetts, 93–135.

Hanka, W., and R. Kind (1994). The GEOFON program, *Ann. Geophys.* **37,** no. 5, 1060–1065.

Hayes, G. P., R. W. Briggs, A. Sladen, E. J. Fielding, C. Prentice, K. Hudnut, P. Mann, F. W. Taylor, A. J. Crone, R. Gold, *et al.* (2010). Complex rupture during the 12 January 2010 Haiti earthquake, *Nature Geosci.* **3,** 800–805.

Hayes, G. P., D. E. McNamara, L. Seidman, and J. Roger (2014). Quantifying potential earthquake and tsunami hazard in the Lesser Antilles subduction zone of the Caribbean region, *Geophys. J. Int.* **196,** 510–521, doi: 10.1093/gji/ggt385.

Hornbach, M. J., N. Braudy, R. W. Briggs, M. Cormier, M. B. Davis, J. B. Diebold, N. Dieudonne, R. Douilly, C. Frohlich, S. P. S. Gulick, *et al.* (2010). High tsunami frequency as a result of combined strike-slip faulting and coastal landslides, *Nature Geosci.* **3,** 783–788.

Intergovernmental Oceanographic Commission (IOC) (2013). *Tsunami and Other Coastal Hazards Warning System for the Caribbean and Adjacent Regions (CARIBE-EWS)*, Implementation Plan 2013–2017, v.2.0, IOC Technical Series No. 78, [online] UNESCO/IOC, available at www.undp.org/.../CesarToro-TsunamiCARIBEEWS.pdf (last accessed July 2014).

Kanamori, H. (1977). The energy release in great earthquakes, *J. Geophys. Res.* **82,** 2881–2987.

Lopez-Venegas, A. M., J. Hornillo, A. Pampell-Manis, V. Huerfano, and A. Mercado (2015). Advanced tsunami numerical simulations and energy considerations by use of 3D-2D coupled models: The October 11, 1918, Mona Passage tsunami, *Pure Appl. Geophys.* **172,** 1679–1698, doi: 10.1007/s00024-014-0988-3.

Mann, P., E. Calais, J.-C. Ruegg, C. DeMets, P. E. Jansma, and G. S. Mattioli (2002). Oblique collision in the northeastern Caribbean from GPS measurements and geological observations, *Tectonics* **21,** doi: 10.1029/2001TC001304.

Mann, P., J.-C. Hippolyte, N. R. Grindlay, and L. J. Abrams (2005). Neotectonics of southern Puerto Rico and its offshore margin, *Geol. Soc. Am. Spec. Pap.* **385,** 173–214.

McCann, W. R., and L. R. Sykes (1984). Subduction of aseismic ridges beneath the Caribbean plate: Implications for the tectonics and seismic potential of the northeastern Caribbean, *J. Geophys. Res.* **89,** 4493–4519.

McGinley, J. R., and D. L. Anderson (1969). Relative amplitudes of *P* and *S* waves as a mantle reconnaissance tool, *Bull. Seismol. Soc. Am.* **59,** 1189–1200.

McNamara, D. E., and R. I. Boaz (2011). PQLX: A seismic data quality control system description, applications, and users manual, *U.S. Geol. Surv. Open-File Rept. 2010–1292*, 41 pp.

McNamara, D. E., and R. P. Buland (2004). Ambient noise levels in the continental United States, *Bull. Seismol. Soc. Am.* **94,** no. 4, 1517–1527.

McNamara, D. E., R. P. Buland, H. M. Benz, and W. Leith (2004). Earthquake detection and location capabilities of the Advanced National Seismic System, *American Geophysical Union, Fall Meeting 2004*, abstract S21A-0264.

McNamara, D. E., C. R. Hutt, L. S. Gee, R. P. Buland, and H. M. Benz (2009). A method to establish seismic noise baselines for automated station assessment, *Seismol. Res. Lett.* **80,** no. 4, 628–637.

McNamara, D., J. McCarthy, and H. Benz (2006). Improving earthquake and tsunami warning for the Caribbean Sea, Gulf of Mexico and the Atlantic Coast, *U.S. Geol. Surv. Fact Sheet, 2006-3012*, 4 pp., (also available at http://pubs.usgs.gov/fs/2006/3012/, last accessed July 2014).

McNamara, D. E., M. Meremonte, J. Z. Maharrey, S.-L. Mildore, J. R. Altidore, D. Anglade, S. E. Hough, D. Given, H. Benz, L. Gee, and A. Frankel (2012). Frequency-dependent seismic attenuation within the Hispaniola Island region of the Caribbean Sea, *Bull. Seismol. Soc. Am.* **102,** no. 2, doi: 10.1785/0120110137.

Motazedian, D., and G. Atkinson (2005). Ground-motion relations for Puerto Rico, in *Active Tectonics and Seismic Hazards of Puerto Rico, the Virgin Islands, and Offshore Areas*, P. Mann (Editor), Geol.l Soc. Am. Spec. Pap. Vol. 385, 61–80.

Parsons, T.,, and E. L. Geist (2009) Tsunami probability in the Caribbean region, *Pure Appl. Geophys.* **165,** 2089–2116.

Peterson, J. (1993). Observation and modeling of seismic background noise, *U.S. Geol. Surv. Tech. Rept., 93-322*, 1–95.

Proenza, X. W., and G. A. Maul (2010). Tsunami hazard and total risk in the Caribbean basin, *Sci. Tsunami Haz.* **29,** no. 2, 70–77.

Robson, G. R. (1964). An earthquake catalogue for the Eastern Caribbean, *Bull. Seismol. Soc. Am.* **54,** 785–832.

Roult, G., and J. P. Montagner (1994). The GEOSCOPE program, *Ann. Geophys.* **37,** no. 5, 1054–1059.

Stein, S., J. F. Engeln, D.A. Weins, K. Fujita, and R. C. Speed (1982). Subduction seismicity and tectonics in the Lesser Antilles arc, *J. Geophys. Res.* **87,** 8642–8664.

Stutzmann, E., R. Geneviève, and L. Astiz (2000). GEOSCOPE station noise levels, *Bull. Seismol. Soc. Am.* **90,** 3690–3701.

ten Brink, U. S., and J. Lin (2004). Stress interaction between subduction earthquakes and forearc strike-slip faults: Modeling and application to the northern Caribbean plate boundary, *J. Geophys. Res.* **109,** no. B12, B12310, doi: 10.1029/2004JB003031.

ten Brink, U. S., H. J. Lee, E. L. Geist, and D. C. Twichell (2009). Assessment of tsunami hazard to the U.S. East Coast using relationships between submarine landslides and earthquakes, *Mar. Geol.* **264,** 65–73.

United Nations Educational, Scientific and Cultural Organization (UNESCO), IOC (2005). *Twenty-Third Session of the Assembly*, Paris, France, 21–30 June 2005.

von Hillebrandt-Andrade, C. (2013). Minimizing Caribbean tsunami risk, *Science* **341,** 966, doi: 10.1126/science.1238943.

Wessel, P., W. H. F. Smith, R. Scharroo, J. Luis, and F. Wobbe (2013). Generic Mapping Tools: Improved version released, *Eos Trans. AGU* **94,** no. 45, 409–410, doi: 10.1002/2013EO450001.

Wiemer, S. (2002). A software package to analyze seismicity: ZMAP, *Seismol. Res. Lett.* **72,** 373–382.

Zahibo, N., E. Pelinovsky, E. A. Okal, A. Yalçiner, C. Kharif, T. Talipova, and A. Kozelkov (2005). The earthquake and tsunami of November 21, 2004 at Les Saintes, Guadeloupe, Lesser Antilles, *Sci. Tsunami Haz.* **23,** 25–39.

Daniel E. McNamara
U.S. Geological Survey
National Earthquake Information Center
1711 Illinois Street
Golden, Colorado 80423 U.S.A.
mcnamara@usgs.gov

Christa von Hillebrandt-Andrade
National Weather Service
Caribbean Tsunami Warning Program
University of Puerto Rico at Mayagüez
259 Boulevard Alfonso Valdés
Mayagüez, Puerto Rico 00680

Jean-Marie Saurel
Institut de Physique du Globe de Paris
Sorbonne Paris Cité
75238 Paris CEDEX 05
France

Victor Huerfano
Puerto Rico Seismic Network
University of Puerto Rico at Mayagüez
259 Boulevard Alfonso Valdés
Mayagüez, Puerto Rico 00680

Lloyd Lynch
Seismic Research Centre
University of the West Indies
St. Augustine
Trinidad & Tobago, West Indies

Published Online 16 December 2015